Self-Assembly Behavior of A-B Diblock and C-D Random Copolymer Mixtures in the Solution State through Mediated Hydrogen Bonding

Chih-Hao Hsu,[†] Shiao-Wei Kuo,*[,‡] Jem-Kun Chen,[§] Fu-Hsiang Ko,[||] Chun-Syong Liao,[†] and Feng-Chih Chang*[,†]

Institute of Applied Chemistry and Institute of Nanotechnology, National Chiao Tung University, Hsin-Chu, Taiwan, Department of Materials and Optoelectronic Science, Center for Nanoscience and Nanotechnology, National Sun Yat-Sen University, Kaohsiung, Taiwan, and Department of Polymer Engineering, National Taiwan University of Science and Technology, Taipei 106, Taiwan

Received December 20, 2007. Revised Manuscript Received May 6, 2008

We have synthesized poly(methyl methacrylate-*b*-4-vinylpyridine) (PMMA-*b*-P4VP) and poly(styrene-*r*-vinylphenol) (PS-*r*-PVPh) copolymers by using anionic and free radical polymerizations, respectively. Well-defined micelles through hydrogen bonding have been prepared by mixing PMMA-*b*-P4VP diblock copolymer and PS-*r*-PVPh random copolymer in a single solvent. Block copolymers were mixed with random copolymers, with various [N]/[OH] ratios (4/1, 2/1, 1/1, and 1/4) in which "[N]/[OH]" represents the molar ratio of pyridine groups on P4VP to hydroxyl groups on PVPh. The presence distribution of PVPh/P4VP and PVPh/PMMA hydrogen bonding depends on the feeding ratio of PVPh to P4VP. When the PVPh content is lower than that of P4VP, hydrogen bonding occurs only between PVPh and P4VP; with excess PVPh, additional hydrogen bonding between PVPh and PMMA would occur. Furthermore, the effect of the solvent quality on the self-assembly behavior of PMMA-*b*-P4VP/PS-*r*-PVPh blends is investigated by considering tetrahydrofuran (THF) and dimethylformamide (DMF) as common solvents. We can mediate the strength of hydrogen bonding in blend systems by adopting different solvents and inducing different morphology transitions.

Introduction

Micellization of amphiphilic block copolymers in the solution state is well documented in scientific literature owing to its potential in various applications, such as drug delivery and stimuli-responsive functional materials of nanodevices.[1–4] Amphiphilic block copolymers can self-assemble in solution to form micelles with various morphologies, including spheres, cylinders, vesicles, wormlike, helical, large compound micelles (LCMs), and many others.[5–12] Micelles of block copolymers, which have a long corona and small core, are termed as "starlike", while the ones with a large core and short corona are termed as "crew-cut".[13] Generally, starlike micelles present as spherical micelles due to their long corona chain; on the contrary, crew-cut micelles could show a wide range of morphologies.[14,15] Parameters to control the morphology of the self-assembled micelles can be divided into two categories: molecular and solution parameters. First, the molecular parameters include the copolymer composition, the chemical characteristics of repeating units, the overall molecular weight, and the molecular structure. In the past decade, manipulating these parameters has been proven to be efficient way of tuning the micelle morphologies.[16,17] The second category, which has been investigated only recently, includes the type of solvent[18] and solvent quality, the solvent/nonsolvent ratio,[19] the copolymer concentration, the pH value, additives such as salts, ions, and homopolymer, and the temperature. The morphology is mainly controlled by a force balance involving three factors: the core-chain stretching, the interfacial energy between the core and outside solvent, and the repulsion among the corona chains. The morphogenic effects of the abovementioned parameters can, in general, be ascribed to their influence on this force balance during the formation of micelles.

Recent advancement has demonstrated that the interpolymer complexation can also induce polymer assembly in solution.[20–28]

* To whom correspondence should be addressed. E-mail: changfc@mail.nctu.edu.tw (F.-C.C.); kuosw@faculty.nsysu.edu.tw (S.-W.K.). Telephone: 886-3-5131512. Fax: 886-3-5131512 (F.-C.C.); 886-7-5254099 (S.-W.K.).

† Institute of Applied Chemistry, National Chiao Tung University.

‡ National Sun Yat-Sen University.

§ National Taiwan University of Science and Technology.

|| Institute of Nanotechnology, National Chiao Tung University.

(1) Gil, E. S.; Hudson, S. A. *Prog. Polym. Sci.* **2004**, *29*, 1173.
(2) Rodriguez-Hernandez, J.; Checot, F.; Gnanou, Y.; Lecommandoux, S. *Prog. Polym. Sci.* **2005**, *30*, 691.
(3) Harada, A.; Kataoka, K. *Prog, Polym. Sci.* **2006**, *31*, 949.
(4) Zhao, Q.; Ni, P. H. *Prog. Chem.* **2006**, *18*, 768.
(5) Van Hest, J. C. M.; Delnoye, D. A.P.; Baars, M. W. P. L.; Van Genderen, M. H. P.; Meijer, E. W. *Science* **1995**, *268*, 1592.
(6) Zhang, L.; Eisenberg, A. *Science* **1995**, *268*, 1728.
(7) Ding, J.; Liu, G. *Macromolecules* **1997**, *30*, 655.
(8) Chan, S. C.; Kuo, S. W.; Lu, C. H.; Fee, H. F.; Chang, F. C. *Polymer* **2007**, *48*, 5059.
(9) Discher, B. M.; Won, Y. Y.; Ege, D. S.; Lee, J. C. M.; Bates, F. S.; Discher, D. E.; Hammer, D. A. *Science* **1999**, *284*, 1143.
(10) Tung, P. H.; Kuo, S. W.; Chen, S. C.; Lin, C. L.; Chang, F. C. *Polymer* **2007**, *48*, 3192.
(11) Antonietti, M.; Föster, S. *Adv. Mater.* **2003**, *15*, 1323.
(12) Jain, S.; Bates, F. S. *Science* **2003**, *300*, 460.
(13) Halperin, A.; Tirrel, M.; Lodge, T. P. *Adv. Polym. Sci.* **1992**, *100*, 31.
(14) Zhang, L.; Eisenberg, A. *J. Am. Chem. Soc.* **1996**, *118*, 3168.
(15) Riegel, I. C.; Eisenberg, A. *Langmuir* **2002**, *18*, 3358.
(16) Chouchair, A.; Eisenberg, A. *Eur. Phys. J. E* **2003**, *10*, 37.
(17) Chen, E.; Xia, Y.; Graham, M. J.; Foster, M. D.; Mi, Y.; Wu, W.; Cheng, S. Z. D. *Chem. Mater.* **2003**, *15*, 2129.
(18) Riegel, I. C.; Samios, D.; Petzhold, C. L.; Eisenberg, A. *Polymer* **2003**, *44*, 2117.
(19) Bhargava, P.; Zheng, J. X.; Li, P.; Quirk, R. P.; Harris, F. W.; Cheng, S. Z. D. *Macromolecules* **2006**, *39*, 4880.
(20) Gohy, J.-F.; Varshney, S. K.; Jérôme, R. *Macromolecules* **2001**, *34*, 3361.
(21) Chen, D.; Jiang, M. *Acc. Chem. Res.* **2005**, *38*, 494.
(22) Hu, J.; Liu, G. *Macromolecules* **2005**, *38*, 8058.
(23) Yan, X.; Liu, G.; Hu, J.; Willson, C. G. *Macromolecules* **2006**, *39*, 1906.
(24) Kabanov, A. V.; Bronich, T. K.; Kabanov, V. A.; Yu, K.; Eisenberg, A. *Macromolecules* **1996**, *29*, 6797.
(25) Bronich, T. K.; Kabanov, A. V.; Kabanov, V. A.; Yu, K.; Eisenberg, A. *Macromolecules* **1997**, *30*, 3519.
(26) Lysenko, E. A.; Bronich, T. K.; Eisenberg, A.; Kabanov, V. A.; Kabanov, A. V. *Macromolecules* **1998**, *31*, 4516.
(27) Bronich, T. K.; Popov, A. M.; Eisenberg, A.; Kabanov, V. A.; Kabanov, A. V. *Langmuir* **2000**, *16*, 481.
(28) Solomatin, S. V.; Bronich, T. K.; Bargar, T. W.; Eisenberg, A.; Kabanov, V. A.; Kabanov, A. V. *Langmuir* **2003**, *19*, 8069.

10.1021/la703960g CCC: $40.75
Published on Web 07/01/2008

An interpolymer complexation can change significantly in terms of the polymer solubility and conformation, which facilitates the intercomplex aggregation. The interactions can be electrostatic interaction,[29] hydrogen bonding,[30–33] and so forth. Usually, micellization of amphiphilic block copolymers in block-selective solvents is the most popular way to prepare micelles. The micelles are usually prepared first by dissolving the block copolymer in a common solvent and then adding a block-selective solvent into the block copolymer solution and dialyzing against a block-selective solvent to remove the common solvent at last. Besides micellization of amphiphilic block copolymers in block-selective solvents, another method to prepare micelles in common solvents through noncovalent hydrogen bonding or electrostatic interaction is also proposed.[29,31] For example, Jiang et al. prepared spherical micellar aggregates by simply mixing poly(styrene-*b*-methyl methacrylate) (PS-*b*-PMMA) and poly{styrene-*co*-[*p*-(2,2,2-trifluoro-1-hydroxyl-1-trifluoromethyl)ethyl-α-emthylstyrene]} (PSOH) in a common solvent of toluene through hydrogen bonding between the pyridine groups and hydroxyl groups.[30]

Herein, we study the comicellization of the diblock copolymer poly(methyl methacrylate-*b*-4-vinyl pyridine) (PMMA-*b*-P4VP) and random copolymer poly(styrene-*r*-vinylphenol) (PS-*r*-PVPh) in nonselective solvents, tetrahydrofuran (THF) and dimethylformamide (DMF), through hydrogen bonding between the hydroxyl groups on PVPh and pyridine groups on P4VP. Furthermore, when the PVPh content is lower than that of P4VP, hydrogen bonding occurs only between PVPh and P4VP; with excess PVPh, additional hydrogen bonding between PVPh and PMMA would occur. It is not easy to construct well-defined micelles involving random amphiphilic copolymers due to their irregularity, and thus, there are extremely few reports discussing this matter.[30,34] However, polystyrene segments in the random copolymer can act as dilute segments to decrease the intramolecular screening and functional-group accessibility effects[35,36] and consequently promise a sufficient hydrogen-bonding complexation. In addition, we can control the strength of hydrogen bonding through mediating the solvent quality; thus, we investigate the solution state self-assembly behavior in both THF and DMF to comprehend the effect of solvent quality on morphology.

Experimental Section

Synthesis of PMMA-*b*-P4VP by Anionic Polymerization. The diblock copolymer poly(methyl methacrylate-*b*-4-vinylpyridine) (PMMA-*b*-P4VP) was synthesized by sequential anionic polymerization of methyl methacrylate followed by 4-vinylpyridine under an inert atmosphere in THF, which was purified by distillation under argon from the red solution obtained by diphenylhexyllithium (produced by the reaction of 1,1-diphenylethylene and *n*-BuLi). *sec*-Butyl lithium was used as the initiator, and degassed methyl alcohol was used as the terminator at −78 °C. Methyl methacrylate and 4-vinylpyridine monomers were distilled from finely ground CaH_2 before use. 4-Vinylpyridine monomer was polymerized first for 2 h, and then an aliquot of poly(4-vinylpyridine) was isolated for analysis after termination with degassed methanol. Methyl methacrylate monomer was then introduced into the reactor, and the reaction was terminated with degassed methanol after 2 h. The product was precipitated in methanol and dried in a vacuum oven, and then poly(methyl methacrylate-*b*-vinylpyridine) had been polymerized completely.

Table 1. Molecular Characterization of PMMA-*b*-P4VP and PS-*r*-PVPh Copolymers

copolymer	repeat unit[a]	M_n[b]	M_w/M_n[b]
PMMA-*b*-P4VP	157−51	15 700−5300	1.1
PS-*r*-PVPh	42−52	4300−6200	2.1

[a] Obtained from ^{1}H NMR measurement. [b] Obtained from GPC analysis.

Synthesis of PS-*r*-PVPh by Free Radical Polymerization. The random copolymer poly(styrene-*r*-vinylphenol) (PS-*r*-PVPh) was synthesized by free radical polymerization. Solution copolymerization of styrene with 4-*tert*-butoxystyrene in benzene was performed in glass reaction flasks containing condensers at 70 °C under an argon atmosphere. 2,2′-Azo-*bis*-isobutyronitrile (AIBN) was employed as the initiator, and the mixture was stirred for ∼12 h. The copolymer was purified by repeatedly dissolving in THF and precipitating in a methanol/water mixture (3:7, v/v). The synthesized poly(styrene-*r*-4-*tert*-butoxystyrene) (PS-*r*-P*t*BOS) was dissolved in dioxane at a concentration of 10% (w/v). The solution was then refluxed overnight in the presence of 37% HCl to remove the *tert*-butoxy groups. Before vacuum drying, poly(styrene-*r*-vinylphenol) (PS-*r*-PVPh) was precipitated repeatedly from THF solution into methanol/water and purified by Soxhlet extraction with water for 72 h to remove any residual HCl. The characteristics of the copolymers used in this work are listed in Table 1.

Preparation of PS-*r*-PVPh/PMMA-*b*-P4VP Micelle Solutions. The PMMA-*b*-P4VP block copolymer was dissolved in THF and DMF to make solutions with a concentration of 1 mg/2 mL, and the PS-*r*-PVPh random copolymer was dissolved in THF and DMF to make random copolymer solutions (2 mL) with desired pyridine/hydroxyl molar ratios ([N]/[OH] = 4/1, 2/1, 1/1, 1/2, and 1/4). These solutions were stirred overnight to ensure complete dissolution. To induce self-assembly, block copolymer solutions were added dropwise (∼1.2 μL/s) to the random copolymer solutions gradually. The complexed solutions were stirred for 1 day and stored at room temperature for further experiments.

Characterizations. *Gel Permeation Chromatography.* Molecular weight and molecular weight distributions were determined through gel permeation chromatography (GPC) using a Waters 510 HPLC instrument equipped with a 410 differential refractometer, a refractive index (RI) detector, and three Ultrastyragel columns (100, 500, and 103) connected in series in order of increasing pore size, with DMF as the eluent at a flow rate of 0.6 mL/min. The molecular weight calibration curve was obtained using polystyrene standards.

Infrared Spectroscopy. Fourier transform infrared (FTIR) spectra were recorded at room temperature at a resolution of 1 cm^{-1} on a Nicolet AVATAR 320 FTIR spectrometer using polymer films cast onto KBr pellets from THF or DMF solution and then vacuum-dried. All FTIR spectra were obtained within the range 4000−400 cm^{-1}; 32 scans were collected at a resolution of 1 cm^{-1} and were purged with nitrogen to maintain the dryness of the film.

Transmission Electron Microscopy. For transmission electron microscopy (TEM) studies, a drop of the resulting micelle solution was sprayed onto a copper TEM grid covered with a Formvar supporting film that had been precoated with a thin film of carbon, and the excess solution was blotted away using a atrip of filter paper immediately. All samples were left to dry at room temperature for 1 day before staining. Samples were stained with ruthenium tetraoxide (RuO_4) and then viewed by using a Hitachi H-7500 transmission electron microscope operated with an accelerating voltage of 100 kV. In the TEM image, it is known for several simple cases that P4VP, PVPh, PS, and PMMA show deep, intermediate, light, and very light contrasts, respectively, by RuO_4 staining.

Dynamic Light Scattering. The hydrodynamic radius, R_h, of the micellar complexes was measured by dynamic light scattering (DLS). DLS measurements were performed on a Brookheaven 90 plus model instrument (Brookheaven Instruments Corporation) with a He−Ne

(29) Schrage, S.; Sigel, R.; Schlaad, H. *Macromolecules* **2003**, *36*, 1417.
(30) Liu, S.; Zhu, H.; Zhao, H.; Jiang, M.; Wu, C. *Langmuir* **2000**, *16*, 3712.
(31) Zhang, W.; Shi, L.; Gao, L.; An, Y.; Li, G.; Wu, K.; Liu, Z. *Macromolecules* **2005**, *38*, 899.
(32) Lefevre, N.; Fustin, C. A.; Gohy, J. F. *Langmuir* **2007**, *23*, 4618.
(33) Kuo, S. W.; Tung, P. H.; Lai, C. L.; Jenog, K. U.; Chang, F. C. *Macromol. Rapid Commun.* **2008**, *29*, 229.
(34) Liu, X.; Wu, J.; Kim, J.-S.; Eisenberg, A. *Langmuir* **2006**, *22*, 419.
(35) Kuo, S. W.; Chang, F. C. *J. Polym. Sci., Part B: Polym. Phys.* **2002**, *40*, 1661.
(36) Lin, C. L.; Chen, W. C.; Liao, C. S.; Su, Y. C.; Huang, C. F.; Kuo, S. W.; Chang, F. C. *Macromolecules* **2005**, *38*, 6435.

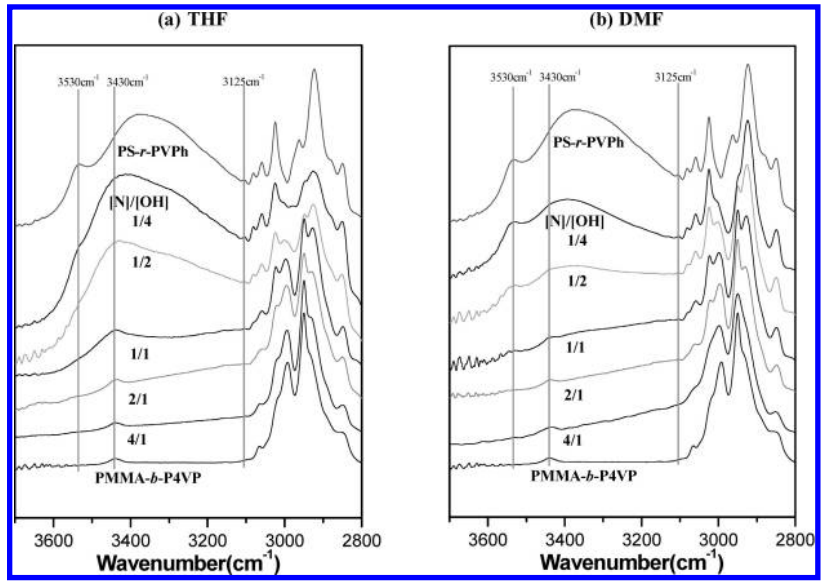

Figure 1. IR spectra, recorded at room temperature, of the region between 2800 and 3700 cm^{-1} of PS-*r*-PVPh and PMMA-*b*-P4VP copolymer blends cast from THF (a) and DMF (b) solutions with various feeding ratios ([N]/[OH).

laser with a power of 35 mW at 632.8 nm. The temperature was controlled at 20 °C, and the measurements were done at an angle of 90°. The polydispersity index (PDI) of the micelles was estimated from the ratio in which Γ_1 and Γ_2 represent the first and second cumulants, respectively. The experimental data have also been analyzed by the CONTIN method.

Results and Discussion

P4VP-*b*-PMMA and PS-*r*-PVPh copolymers were mixed in THF or DMF solvent (both are good solvents for PS and PMMA blocks), and micelles were then formed in different morphologies depending on the feeding ratio ([N]/[OH]). These noncovalently connected polymeric micelles formed by mixtures of PMMA-*b*-P4VP and PS-*r*-PVPh were analyzed by infrared spectroscopy, transmission electron microscopy, and dynamic light scattering.

Hydrogen Bonding in the Blending System. FTIR spectroscopy has been successfully applied in numerous diblock copolymers and blends possessing intermolecular interaction through hydrogen bonding. In addition, it has been found that the hydrogen-bonding complexation is strongly influenced by the solvent used. Figure 1 shows the infrared spectra at a hydroxyl stretching analysis of various compositions of PS-*r*-PVPh/PMMA-*b*-P4VP blends in THF and DMF solutions at room temperature. The spectrum of pure PS-*r*-PVPh shows a broad band at 3360 cm^{-1} and a shoulder at 3525 cm^{-1}, corresponding to the multimer hydrogen-bonded hydroxyl groups and the free hydroxyl groups, respectively. For the polymer film prepared from both THF and DMF solutions, the band (at 3125 cm^{-1}) fraction increases first with increasing P4VP content as a result of the decrease in the fraction of the multimer hydrogen-bonded hydroxyl band; therefore, it is reasonable to assign this band at 3125 cm^{-1} as the hydroxyl group bonded to the pyridine group. Figure 2 shows the infrared spectra at hydroxyl stretching of pure PS-*r*-PVPh and blends with [N]/[OH] ratio = 1/4 polymer film prepared from THF and DMF solutions at room temperature. Now, we focus on the variation of free hydroxyl groups of the blends in THF and DMF. The peak frequency of the hydrogen-bonded hydroxyl group of THF system shifts to a lower wavenumber (3300 cm^{-1}) than the corresponding one of the DMF system, reflecting that the strength of hydrogen bonding between PVPh and P4VP in THF is greater than that in DMF. In addition, we observe that the hydroxyl stretching band of the

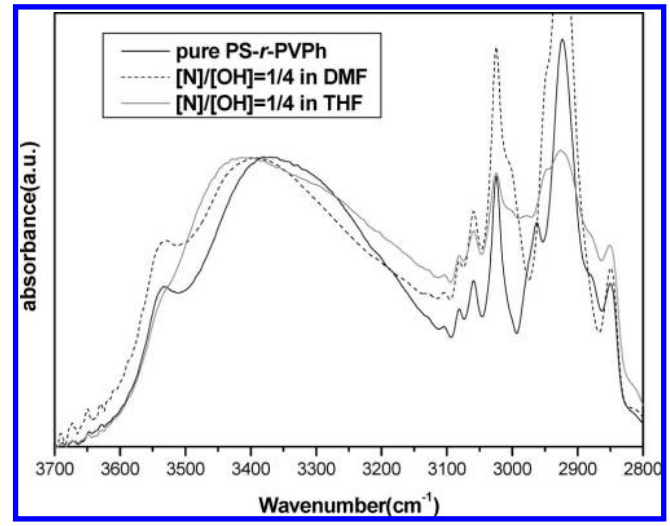

Figure 2. IR spectra, recorded at room temperature, of the region between 2800 and 3700 cm^{-1} of PS-*r*-PVPh and PMMA-*b*-P4VP copolymer blends ([N]/[OH = 1/4) cast from THF and DMF solutions.

THF system is broader and more asymmetric than the corresponding band of the DMF system. Coleman et al. compared the frequency difference ($\Delta\nu$) between the hydrogen-bonded hydroxyl absorption and the free hydroxyl absorption to access the average strength of the intermolecular interaction.[37] Therefore, we can conclude that the strength of the hydroxyl−pyridine interaction is clearly stronger than that of hydrogen−hydrogen, and the hydrogen−carbonyl interaction is the weakest.

However, the overtone of carbonyl stretching of PMMA is observed at 3430 cm^{-1} especially at high PMMA content. The distribution of hydroxyl groups cannot be quantitatively described because of this overlap of the overtone in the hydroxyl stretching. Thus, we consider another region of the FTIR spectra to confirm the interaction between PVPh and PMMA. Figure 3 presents the FTIR spectra of the carbonyl stretching region at room temperature ranging from 1680 to 1780 cm^{-1} for different compositions of PMMA-*b*-P4VP/PS-*r*-PVPh polymer blend films prepared from THF and DMF. For the MMA units, the FTIR carbonyl stretching

(37) Moskala, E. J.; Varnell, D. F.; Coleman, M. M. *Polymer* **1985**, *26*, 228.

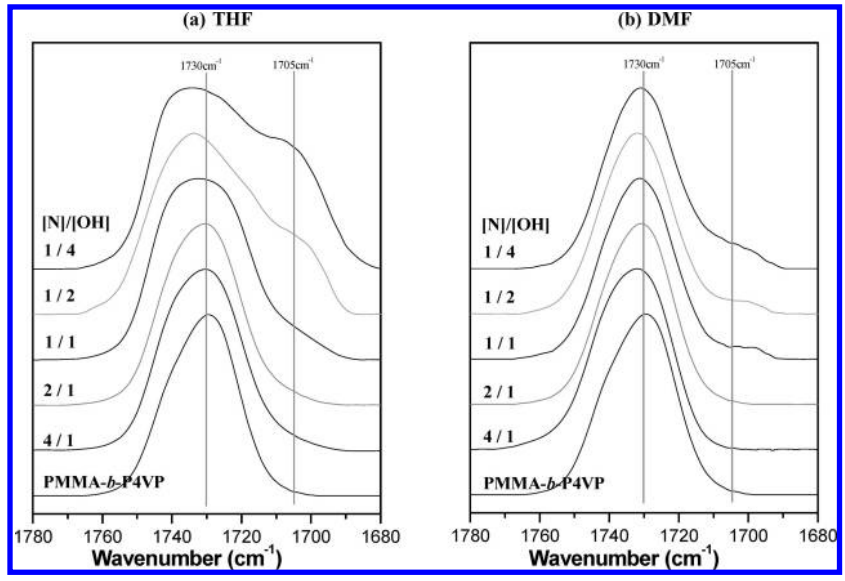

Figure 3. IR spectra, recorded at room temperature, of the region between 1680 and 1780 cm^{-1} of P4VP-*b*-PMMA/PS-*r*-PVPh copolymer blends cast from THF and DMF solutions.

absorptions by free and hydrogen-bonded carbonyl groups are at 1730 and 1705 cm^{-1}, respectively.[4] As the PVPh content in the blend increases, different characteristics of carbonyl stretching absorption in THF and DMF system have been identified. In THF system, a shoulder appears at 1705 cm^{-1} only when the PVPh content is superior to P4VP in the blend, reflecting the presence of intermolecular hydrogen bonding between the PVPh and PMMA blocks at [N]/[OH] = 1/1, 1/2, and 1/4. This result also implies that the hydrogen-bonding between PVPh and P4VP is stronger than that between PVPh and PMMA, so that the PMMA carbonyl groups interact insignificantly with PVPh only when the [N]/[OH] ratio is less than 1/1. In contrast, the carbonyl stretching absorption in the DMF system undergoes a very slight alteration at 1705 cm^{-1} with increasing PVPh content. This result implies that the residual PVPh at [N]/[OH] = 1/2 and 1/4 would not prefer to interact with PMMA. As already stated, the strength of hydroxyl−carbonyl is the weakest among the distribution of hydrogen bonding. Thus, we can roughly assume that competitive hydrogen-bonding formations exist between hydroxyl−carbonyl and hydroxyl−DMF, while the hydroxyl−DMF is more favorable.

A procedure of least-squares curve fitting can be applied to the carbonyl stretching region using two Gaussian bands, and a quantitative measure of the fraction of "free" carbonyl groups can be readily determined using the value of the absorptivity coefficient 1.5, which is the ratio of these two bands, the free and hydrogen-bonded carbonyl groups in an ester group. The fraction of the hydrogen-bonded carbonyl group can be calculated as shown below:

$$f_b^{C=O} = \frac{A_b/1.5}{A_b/1.5 + A_f} \quad (1)$$

A_b is the peak area of the hydrogen-bonded carbonyl absorption, and A_f is the peak area of the free carbonyl absorption. $f_b^{C=O}$ is the fraction of hydrogen-bonded carbonyl groups. The curve fitting results are summarized in Table 2. From Table 2, we can quantitatively observe that the fraction of hydrogen-bonded carbonyl groups in the THF system reaches 22% but only 4.9% in the DMF system.

Besides the hydroxyl stretching region, some characteristic modes of the pyridine ring are sensitive to hydrogen-bonding interaction. These modes including 1590, 1050, 993, and 625 cm^{-1} shift to 1600, 1067, 1011, and 634 cm^{-1}, respectively, after forming hydrogen-bonding interactions with the carboxylic acid groups of poly(ethylene-*co*-methacrylic acid).[38] Unfortunately, the bands at 1590 cm^{-1} for P4VP are difficult to analyze due to overlapping with the 1600 cm^{-1} band from PVPh. Therefore, only the band at 993 cm^{-1} can be used to analyze the hydrogen-bonding interactions between the hydroxyl group of PVPh and the pyridine group of P4VP. Figure 4 shows the scale-expanded infrared spectra in the range 970−1030 cm^{-1} measured at room temperature for pure PVPh, P4VP, and copolymer blends with various [N]/[OH] ratios. Pure P4VP has a characteristic band at 993 cm^{-1}, corresponding to the pure pyridine ring absorption. Pure PVPh does not absorb at 993 cm^{-1} but has a band at 1013 cm^{-1}. These two bands are well resolved without overlapping. Upon complexation of PVPh with P4VP, a new band appearing at 1005 cm^{-1} is assigned to the hydrogen-bonded pyridine rings of P4VP, which has been earlier demonstrated in a diblock copolymer PVPh-*b*-P4VP.[39] A band at 1005 cm^{-1} is observed in both THF and DMF, indicating the existence of complexation between PVPh and P4VP, comicellizaion driving force, in both nonselective solvents.

Table 2. Carbonyl Group Curve-Fitting Results of the PS-*r*-PVPh/PMMA-*b*-P4VP Blends in THF and DMF[a]

		ν_f (cm^{-1})	A_f (%)	ν_b (cm^{-1})	A_b (%)	f_b (%)
THF	4/1	1730	100		0	0
	2/1	1730	100		0	0
	1/1	1730	90.7	1705	9.3	6.4
	1/2	1730	77.9	1705	22.1	15.9
	1/4	1730	70.0	1705	30.0	22.2
DMF	4/1	1730	100		0	0
	2/1	1730	100		0	0
	1/1	1731	98.5	1703	1.5	1.0
	1/2	1732	97.3	1703	2.7	1.8
	1/4	1731	92.8	1704	7.2	4.9

[a] ν_f = wavenumber of free C=O of PMMA, ν_b = wavenumber of hydrogen-bonded carbonyl of PMMA, A_f = free C=O area fraction of PMMA, A_b = free C=O area fraction of hydrogen-bonded PMMA, and f_b = fraction of hydrogen-bonded of PMMA.

(38) Lee, Y. J.; Painter, P. C.; Coleman, M. M. *Macromolecules* **1988**, *21*, 954.
(39) Kuo, S. W.; Tung, P. H.; Chang, F. C. *Macromolecules* **2006**, *39*, 9388.

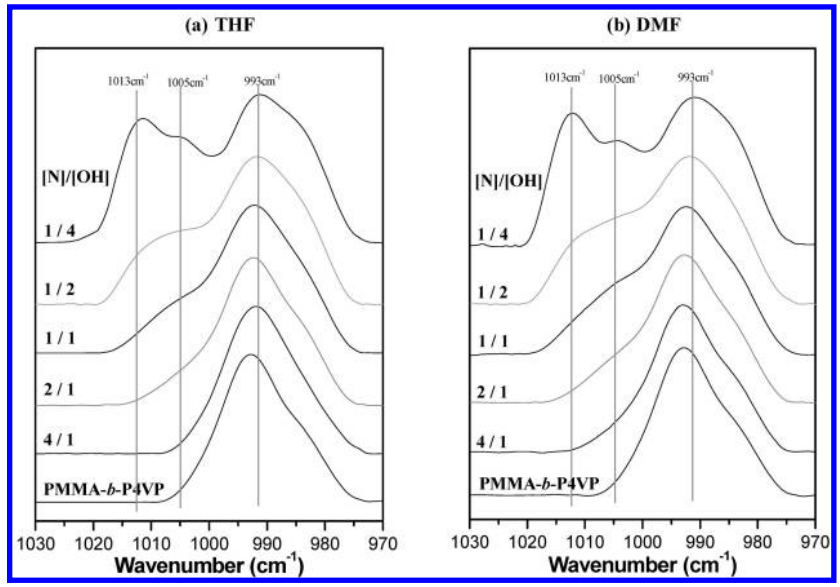

Figure 4. IR spectra, recorded at room temperature, of the region between 970 and 1030 cm^{-1} of P4VP-*b*-PMMA/PS-*r*-PVPh copolymer blends cast from THF and DMF solutions.

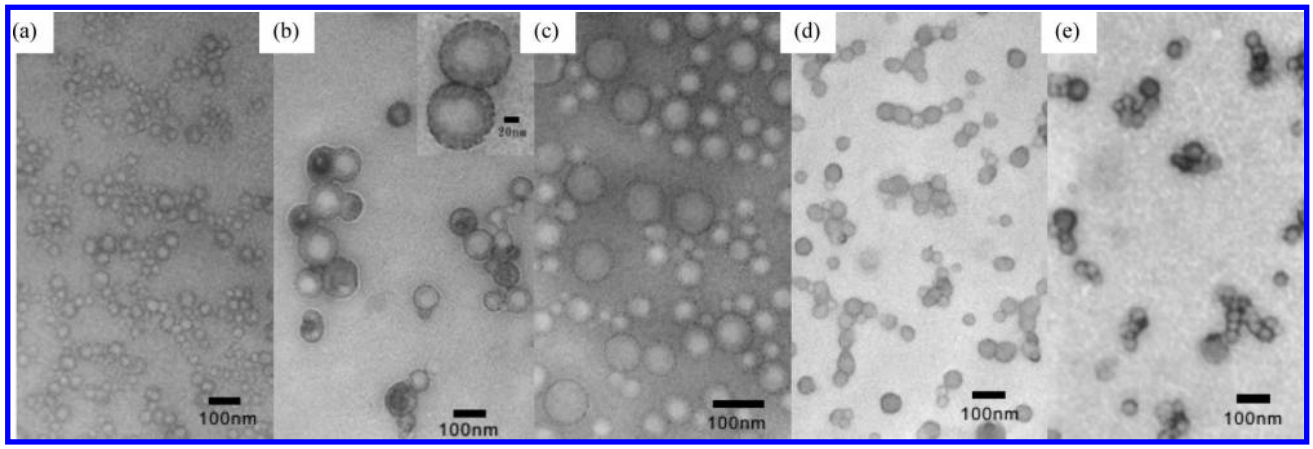

Figure 5. TEM images of PS-*r*-PVPh/PMMA-*b*-P4VP blends in THF at (a) [N]/[OH] = 4/1, (b) [N]/[OH] = 2/1, (c) [N]/[OH] = 1/1, (d) [N]/[OH] = 1/2, and (e) [N]/[OH] = 1/4.

Structures of PMMA-*b*-P4VP/ PS-*r*-PVPh Micelles in THF Solution. Figure 5 shows that, with increasing PVPh content, the morphology of the aggregates changes from vesicles to spheres. Vesicles with a core thickness of ~10 nm are the only morphology seen (Figure 5a,b) when the [N]/[OH ratios are 4/1 and 2/1. As the P4VP block with M_n = 5300 has an unperturbed end-to-end distance of ~5 nm, the core thickness of 10 nm indicates that the membrane is a bilayer or a partially interdigitated structure (Scheme 1) with the P4VP blocks extended to a certain extent when the P4VP/PVPh complex is formed.

At [N]/[OH ratios of 4/1 and 2/1, the high interchain hydrogen bonding between copolymer chains tends to induce polymer complex aggregation in the form of a vesicle with a PVPh/P4VP core surrounded by PMMA blocks. According to the conventional concepts of a star-micelle, vesicles should not be observed in our system, where the corona-formed soluble chain is much longer than the core-formed insoluble chain. The formation of vesicles is, most likely, a result of the strong interaction between PVPh and P4VP. As already confirmed, the complex ability of PVPh/P4VP in THF is better than that in DMF. For the mixture of P4VP and PVPh in THF, a fairly long continuous linear succession of hydrogen bonds between monomer units of P4VP and PVPh may result in a ladderlike

Scheme 1. Schematic Illustration of a Bilayer Vesicle of PS-*r*-PVPh/PMMA-*b*-P4VP

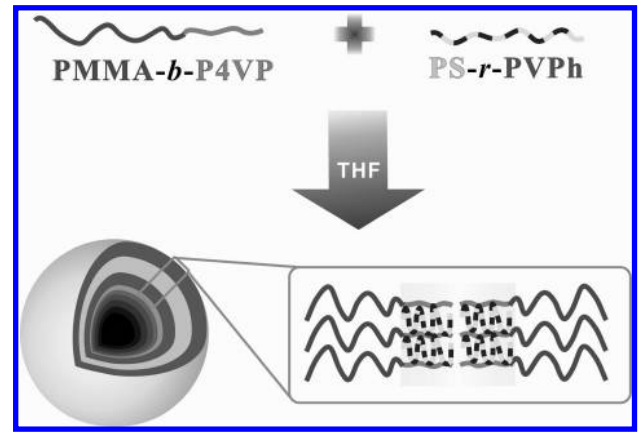

structure. According to Antonietti and Föster,[11] such a complexation will restrict the intermolecular conformation and lead to a preferred parallel alignment. The parallel alignment of P4VP and PS-*r*-PVPh chains in the core forces the aggregates to adopt a vesicle morphology.

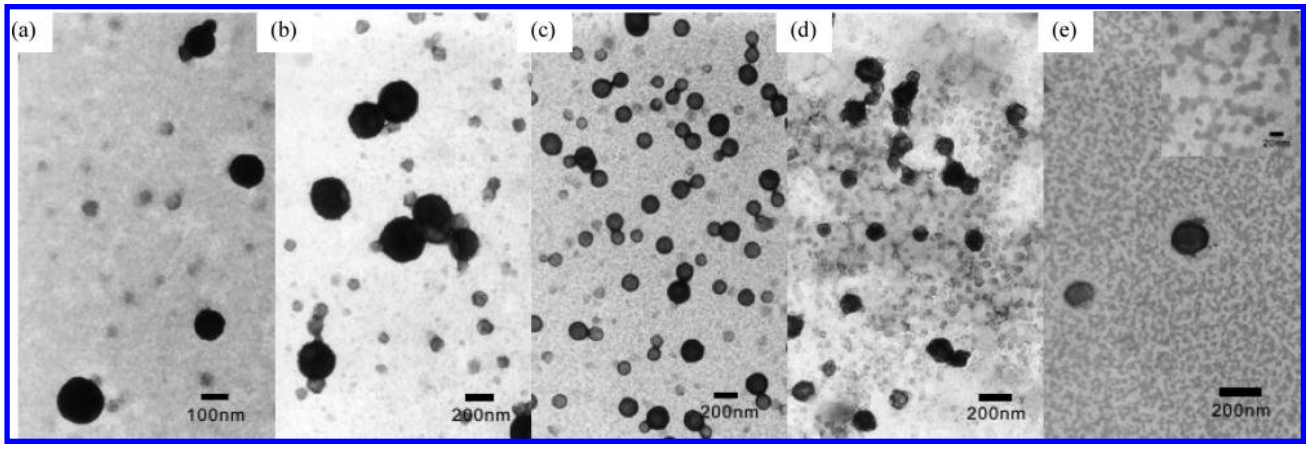

Figure 6. TEM images of PS-*r*-PVPh/PMMA-*b*-P4VP blends in THF at (a) [N]/[OH] = 4/1, (b) [N]/[OH] = 2/1, (c) [N]/[OH] = 1/1, (d) [N]/[OH] = 1/2, and (e) [N]/[OH] = 1/4.

Scheme 2. Schematic Illustration of Complex Section Change in the Morphology Transition from Vesicles to Spheres

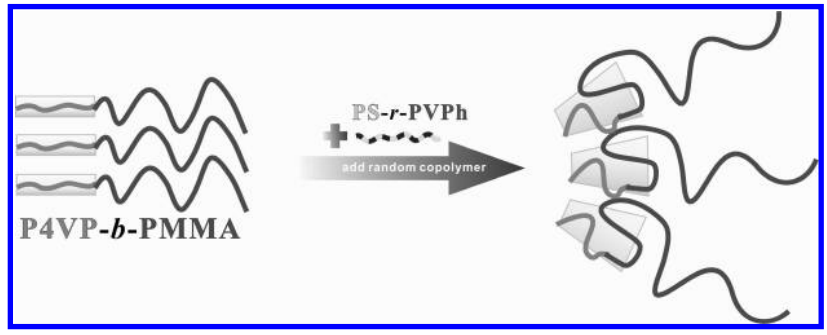

Scheme 3. Schematic Illustration of Mechanism of Morphology Transition from Compound Spheres to Primary Spheres

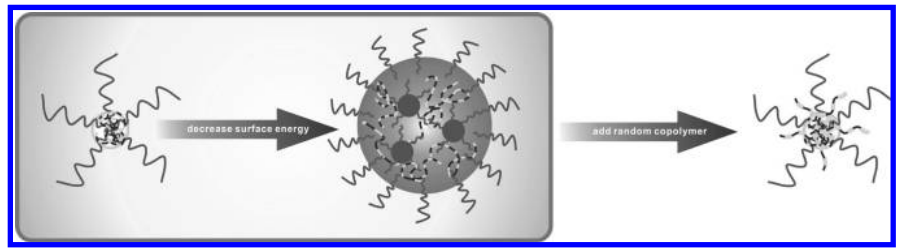

As the content of PS-*r*-PVPh increases, more residual hydroxyls of PVPh can complex with the carbonyl groups of PMMA. In this situation, the PVPh/PMMA complex also acts as a core-formed chain just like the PVPh/P4VP complex; however, the complex ability of PVPh/PMMA is not strong enough to restrict the intermolecular conformation and lead to a parallel alignment. Thus, the dimension of the core formed by PVPh/PMMA is looser than that formed by PVPh/P4VP, and the asymmetric core structure in Scheme 2 means a decrease of packing parameter. Typically, the packing parameter of an amphiphilic copolymer increases as the morphology changes from sphere to cylinder, and to bilayer. Vesicle formation is, therefore, not favored because the tendency to form closed bilayer structures (precursors of vesicles) highly decreases as the packing parameter decreases. As a result, both vesicles and spheres are observed (Figure 5c) when the [N]/[OH] ratio is equal to 1/1, and a further increase in random copolymer leads to the observation of only spheres (Figure 5d,e) at [N]/[OH] = 1/2 and 1/4.

Structures of PMMA-*b*-P4VP/ PS-*r*-PVPh Micelles in DMF Solution. Figure 6 shows a comparison of micrographs of aggregates formed from blends with various [N]/[OH] ratios in DMF. Compound sphere is the main morphology at [N]/[OH] = 4/1 (Figure 6a). Increasing the PVPh content of the blend further to [N]/[OH] = 2/1, 1/1, and 1/2, compound spheres accompanied by the appearance of spheres (Figure 6b−d) are observed. Finally, at [N]/[OH] = 1/4, mainly primary spherical micelles (Figure 6e) are observed.

Table 3. DLS Results and TEM Morphology for the PS-*r*-PVPh/ PMMA-*b*-P4VP Blends in THF and DMF

solvent	[N]/[OH] Ratio	DLSHydrodynamic diameter (nm)	DLS polydispersity	TEM morphology
THF	4/1	67	0.13	vesicle
	2/1	75	0.12	vesicle
	1/1	82	0.07	vesicle + sphere
	1/2	75	0.07	sphere
	1/4	66	0.12	sphere
DMF	4/1	13, 157	0.29	sphere
	2/1	8, 135	0.25	sphere
	1/1	7, 16, 114	0.15	sphere
	1/2	10, 75	0.12	Sphere
	1/4	10, 100	0.11	Sphere

In DMF, which is a better proton accepter solvent than THF for the hydroxyl groups, DMF solvent molecules can also

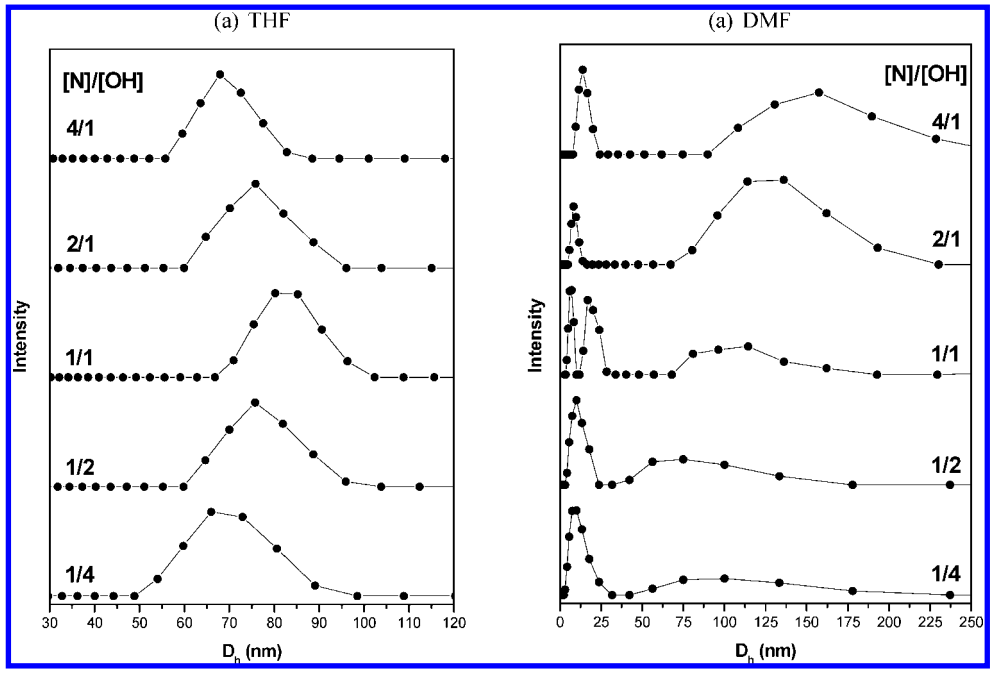

Figure 7. Intensity-weighted hydrodynamic diameter distribution of PS-*r*-PVPh/PMMA-*b*-P4VP blends with various [N]/[OH] ratios at 20 °C in THF (a) and DMF (b).

participate in hydrogen-bonding interaction and solvate many hydroxyl groups as free OH groups, which has been demonstrated by FTIR; therefore, pyridine groups of P4VP cannot complex with hydroxyl groups of PVPh in DMF as sufficiently as they do in THF. Thus, it is not surprising that no vesicles are observed because the complexation in DMF cannot lead to core chains in a preferred parallel alignment.

Large compound micelles (LCMs) are believed to be composed of an assembly of reverse micelles. Generally, aggregates with short hydrophobic chains (crew-cut micelles) possess a greater possibility to form LCMs, because short hydrophobic chains could easily form pockets in the hydrophilic chain-rich phase. However, in our system, corona chains are almost three times the length of the core chains (starlike micelles). Thus, these observed compound spheres should be formed in the other mechanism. The most likely mechanism is that the formed primary spheres with minor random copolymers possess high interfacial energy (Scheme 3) and make the system unstable. Due to the core chain stretching being confined by the complexation between PVPh and P4VP, the core chain stretching and consequently the core radius (R_{core}) of the primary spheres are fixed. The system in DMF cannot decrease the total interfacial energy by means of increasing R_{core}; thus, the system may choose to form compound spheres to decrease the total interfacial energy because compound spheres possess fewer total interfaces between the core chains and solvent molecules.

As mentioned before, the complexation between PVPh and PMMA is very slight; therefore, as the [N]/[OH] ratio is less than 1/1, excess random copolymer segments would rather extend from the core than complex with PMMA. From the TEM pictures, it appears, qualitatively, that increasing the PVPh content from [N]/[OH] = 4/1 to 1/4 results in fewer compound spheres and more primary spherical micelles. The apparent change in the ratio of spheres to compound spheres can be explained by looking at the compositions of the mixture. As the random copolymer content increases, there are more short chains (random copolymer chains) in the corona; these short chains could decrease the interfacial energy to stabilize the spherical micelles and result in fewer compound spheres.

Hydrodynamic Diameter Distribution of PMMA-*b*-P4VP/PS-*r*-PVPh Micelles. DLS results (Figure 7a) show that the hydrodynamic diameter ($D_{h)}$ of the micellar complexes in THF increases from 69 to 84 nm and then decreases to 67 nm when the PVPh molar fraction increases from [N]/[OH] = 4/1 to 1/4 (Table 3). A possible consequence of the change in aggregate size is described below: First, as the PVPh molar fraction ranges from [N]/[OH] = 4/1 to 1/1, vesicle wall thicknesses do not appear to change but vesicle sizes increase from 69 to 84 nm. The reason for the increase in vesicle sizes in response to the increase PVPh content is probably related to the increase in the interfacial energy in the system, which would drive the system to decrease the total interfacial energy. Because the degree of complexation between P4VP and PVPh in the core increases with increasing PVPh molar fraction, the solubility of the core for the THF solution decreases gradually and consequently increases interfacial energy in the system. Second, as the PVPh molar fraction ranges from [N]/[OH] = 1/2 to 1/4, spherical aggregate sizes change from 75 to 66 nm. Considering that the aggregation number of spherical aggregates is constant, the core of spherical aggregates accommodates a constant amount of P4VP and PVPh segments. Spherical aggregates at [N]/[OH] = 1/4 are smaller compared to those at [N]/[OH] = 1/2 because partial coronal PMMA chains are grabbed by excess PVPh segments at [N]/[OH] = 1/4, decreasing the degree of corona chain extension and consequently decreasing the hydrodynamic diameter of spherical aggregates.

Additionally, spherical aggregates with a core that is composed of fully stretched P4VP chains are estimated to be around 10 nm, because each fully stretched core chain with 50 repeat units of 4VP is around 5 nm; however, the spherical aggregates (~67 nm) observed at [N]/[OH] = 1/4 in THF are greater than those estimated to be composed of fully stretched core chains in the core. This phenomenon might be attributed to the complexation between PMMA and PVPh in the condition that PVPh is the majority in the blends; thus, partial PMMA-*b*-P4VP chains can fully permeate into a complexed core of spherical aggregates and consequently enlarge the size of core.

DLS results (Figure 7b) show that the hydrodynamic diameter distributions of the micellar complexes in DMF are bimodal. The bimodal distributions correspond to primary spheres (∼10 nm) and compound spheres (80−150 nm) as shown in the TEM pictures. Additionally, the intensity of the compound sphere increases as the PVPh content increases at the [N]/[OH] ratio between 4/1 and 2/1, and then the intensity decreases in the [N]/[OH] ratio ranging from 2/1 to 1/4. First, the increase of the compound sphere intensity is attributed to the increasing number of P4VP/PVPh complexes. The higher the degree of complexation in the core, the higher the interfacial energy is; thus, the intensity of the compound sphere at [N]/[OH] = 2/1 is greater than that at [N]/[OH] = 4/1. Second, the decrease of compound sphere intensity results from the same reason for the presence of medium spheres: the random copolymer chains insert into the interface, making the primary sphere stable, and consequently, the compound sphere intensity decreases.

Conclusions

Hydrogen bonding between diblock copolymer PMMA-*b*-P4VP and random copolymer PS-*r*-PVPh in nonselective solvents results in well-defined micelles with the core and shell being composed of insoluble PVPh/P4VP complexes and soluble PMMA blocks, respectively. FTIR spectra provided evidence that the strength of PVPh/P4VP is greater than PVPh/PMMA complexes, which results in different morphologies in THF and DMF. Obvious complexation between excessive PVPh and PMMA in the THF system and only very slight complexation in the DMF system have also been confirmed by FTIR spectra.

In THF, when PS-*r*-PVPh is the minor component in the blends, parallel alignment of P4VP chains in the core forces the aggregates to adopt a vesicle morphology; when PS-*r*-PVPh is the major component in the blends, PVPh/PMMA complexs dilute and disturb the compact structure of PVPh/P4VP, driving the aggregates' morphology into spheres. In DMF, when PS-*r*-PVPh is the minor component in the blends, the primary spheres are instable and easily form compound sheres; when PS-*r*-PVPh is the major component in the blends, unreacted PS-*r*-PVPh chains can decrease the interfacial energy and further stabilize primary spheres. All the results show that well-defined micelles can be obtained in nonselective solvents through hydrogen bonding and that the strength of hydrogen bonding can be mediated by adopting different solvents to affect the self-assembly behavior.

Acknowledgment. This work was supported financially by the National Science Council, Taiwan, Republic of China, under Contract Nos. NSC-96-2120-M-009-009 and NSC-96-2218-E-110-008.

LA703960G